

# Test and simulation of superconducting magnetic bearings

Guilherme Goncalves Sotelo, Rubens de Andrade, Jr. and Antonio Carlos Ferreira

**Abstract**—This work presents the study of superconducting magnetic bearings (SMB). Two SMB prototypes were constructed using Nd-Fe-B magnets rotors (each one having approximately 80mm of external diameter) and a 75mm diameter YBCO disc. The magnetic rotors of the SMB prototypes were manufactured in two different topologies: flux shaper and axially magnetized rings. Bean's critical state model is applied to simulate those SMBs. The model was implemented using magnetostatic solutions calculated by finite element method (to solve the problem in space) and finite difference method (to solve the problem in time). Simulated and measured results were very similar, showing the applied simulation model is efficient to this purpose.

**Index Terms**—Superconducting Magnetic Bearing, Critical State Model.

## I. INTRODUCTION

The investigation of devices that can reduce the energy loss caused by friction in rotation shafts at high speed ( $> 10.000$  rpm) is important for systems where the efficiency is primordial. In this context, the superconducting magnetic bearing (SMB) can be considered a promising solution [1]. The advantages of SMBs are high levitation pressure (up to  $4 \text{ N/mm}^2$ ) and stiffness [2], total stability in all the directions without the need of a control system, reduced friction loss (no contact) and reduced maintenance cost. However, an amount of energy must be spent to cool the high temperature superconductor (HTS) and the SMB's project presents some difficulty because of the high non linearity involved in the levitation force. The literature presents several models to simulate the levitation force between a superconductor and an external field. Most of them are based on the critical state model [3] [4]. To simulate complex geometries the best option is to use models based on the finite element method (FEM) [5]. In this work, the model presented in [6] is applied to simulate relatively complex SMB geometries. Two prototypes of SMB were constructed with a 75mm diameter HTS disk grown by seeded melt textured and 80mm diameter magnetic rotors (having 2 different magnetic arrangement).

## II. SUPERCONDUCTOR MODELLING

The high non-linearity involved in the relationship between the electric field and the current density (E-J relation) inside the superconductor, makes it necessary to adopt a numerical method to solve the problem. To reduce the number of degrees

of freedom of the problem, it is adopted a formulation based on the magnetic vector potential ( $\vec{A}$ ) and scalar electrical potential ( $V$ ), known as  $A-V$  formulation. With this formulation, in the simulations presented in this work, the only degree of freedom is  $A_\phi$ , the magnetic vector potential in the azimuthal direction ( $\phi$ ). In the solution of problems with axial symmetry, the electric field, the electric current density and magnetic vector potential are on the same direction, presenting only one non null component in the direction  $\phi$ . This means that  $\vec{A} = A_\phi$ ,  $\vec{E} = E_\phi$  and  $\vec{J} = J_\phi$ . From Faraday's law, the electric field inside the superconductor can be calculated as:

$$E_\phi = -\frac{\partial A_{\phi Tot}}{\partial t} - \nabla V = -\frac{\partial A_{\phi sc}}{\partial t} - \frac{\partial A_{\phi Ext}}{\partial t} - \nabla V, \quad (1)$$

where the subscripts  $Ext$  and  $SC$  mean the external and superconductor contributions, respectively. The gradient of the electric scalar potential can have only one component along  $\phi$  direction. As the electric scalar potential has a constant value in the symmetry plane, than  $\nabla V = 0$ . The Poisson equation is used by FEM to solve the spatial problem in terms of magnetic vector potential:

$$\nabla^2 A_{\phi Tot} = -\mu_0 \cdot J_{\phi Tot} = -\mu_0 \cdot (J_{\phi sc} + J_{\phi ext}), \quad (2)$$

The critical state model suggests that the non linear  $E - J$  relationship can be solved as presented in [5]:

$$J_{\phi sc} = J_c(|\vec{B}|) \text{sign}(E) \quad \text{if} \quad E_\phi \neq 0 \quad (3)$$

and

$$\frac{\partial J_{\phi sc}}{\partial t} = 0 \quad \text{if} \quad E_\phi = 0. \quad (4)$$

The function  $\text{sign}(E)$  represents the electric field signal and it has the same direction of the electric current density. In an axisymmetric simulation, function  $\text{sign}$  means that the current density may be in the clockwise or counterclockwise sense.

The methodology applied here to calculate the induced current density inside the superconductor do not attempt to solve interactively equations 1 to 2. First, the spatial solution is obtained in time by FEM (considering all the possible solutions), then the time solution is proceed by finite difference method (FDM), where the movement is included. To find the solution by the critical state model, it is necessary to eliminate  $A_{\phi sc}$  in equations 1 and 2. Considering the type II superconductor as a linear medium ( $B = \mu_0 H$ ) having a screening current, the superposition principle can be applied, as done by [8]. If any external excitation is eliminated ( $J_{\phi ext} = 0$ ) it is possible to rewrite equation 2 as:

$$\nabla^2 A_{\phi sc} = -\mu_0 \cdot J_{\phi sc}. \quad (5)$$

Manuscript received August 15, 2008; This work was supported by the Brazilian agencies Faperj and CNPq.

G.G. Sotelo is with PEE-COPPE/UFRJ, Universidade Federal do Rio de Janeiro and Faculdade Salesiana Maria Auxiliadora (sotelo@coe.ufrj.br); R.de Andrade Jr. and A.C. Ferreira are with Universidade Federal do Rio de Janeiro (randrade@dee.ufrj.br, ferreira@ufrj.br).

Instead of solving equation 5 at each instant of time in the FEM program, it is proposed to solve the magnetic vector potential in the superconductor ( $A_{\phi_{sc}}$ ) as a function of the distribution of the current density in the HTS. The  $A_{\phi_{sc}}$  can be obtained by the G function, where the relation  $A_{\phi_{sc}} = \mu_0 G * J_{\phi_{sc}}$  is obeyed. The G function can be found by two different ways: by the integral form of relation 5 and an appropriated Green function [9] or by matrixes generated by multiple solutions of Poisson equation in a FEM program using adequate boundary conditions [8]. Because it is necessary to simulate complex geometries of magnetic rotors for the SMB, that present non linearity properties, the second option is more appropriate here.

Lets suppose the superconductor mesh has N elements, it will be necessary N solutions of the Poisson equation in the FEM program to complete G. Each collum of the G matrix is composed by a correspondent FEM solution applying a "unity current density" only in the  $i$  element of superconductor. For all the others elements, the electric current density must be null. The magnetic vector potential calculated values must be divided by the "unity applied J" to compose the  $i$ -th collum of a matrix denominated  $[M]_{N \times N}$ , since  $[M] = \mu_0 G$ . Grouping all the N solutions, for the N elements of the superconductor mesh, it is possible to write the following equation applying the superposition principle:

$$[A_{\phi_{sc}}]_{N \times 1} = [M]_{N \times N} \times [J_{\phi_{sc}}]_{N \times 1}. \quad (6)$$

An example of how to create the  $[M]$  matrix for a 4 element HTS mesh in the FEM program is presented in figure 1.

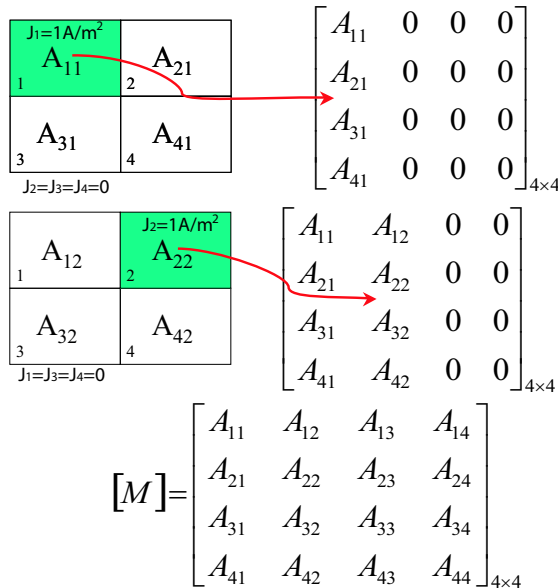


Fig. 1. Example of a 4 elements HTS mesh to create  $[M]$ .

In spite of needing N solutions of Poisson equation in the MEF program, this procedure is made only once for the same superconductor geometry. If the critical current density need to be changed, it is not necessary to create  $[M]$  again. On the other hand, if it is desired to simulate other HTS geometry, all the procedure described above must be applied again.

Substituting equation 6 in relation 1 and applying the FDM to solve the problem in time, the electric field can be found by the A-V formulation:

$$[E_{AV}^t] = [E_{\phi}^t] = - \frac{[M] \times ([J_{\phi_{sc}}^t] - [J_{\phi_{sc}}^{t-1}])}{\Delta t} - \frac{[A_{\phi_{ext}}^t] - [A_{\phi_{ext}}^{t-1}]}{\Delta t}. \quad (7)$$

The objective of calculating the electric field in equation 7 is to find the electrical current density distribution inside the HTS in time  $t$  ( $[J_{\phi_{sc}}^t]$ ). The non-linearity of the problem will be inserted applying the calculation of the electric field by the critical state model ( $E_{EC}$ ). Now it is made the inversion of the problem presented by equations 3 and 4. Considering that the electric field is null if the current density modulus is inferior to  $|J_c|$ . The electric field calculated in the element by the critical state model is assumed non null if the magnitude of the critical current density is equal to  $J_c$ . And so, the electric field obtained by the critical state model ( $E_{EC}$ ) will be obtained individually for each element  $e$  of the HTS mesh, by the following relation:

$$E_{EC}^t(e) = E_{\phi}^t(e) \quad \text{if} \quad |J_{\phi_{sc}}^t(e)| = J_c, \quad (8)$$

$$E_{EC}^t(e) = 0 \quad \text{if} \quad 0 < |J_{\phi_{sc}}^t(e)| < J_c. \quad (9)$$

The difference between the electric field calculated by the A-V ( $E_{AV}$  in the equation 7) and the electric field calculated by the critical state model formulation ( $E_{EC}$  in equations 8 and 9) must be null. To solve the problem, it will be created a collum matrix  $[ERROR]_{N \times 1}$ , which will be minimized for each relative position between the magnetic rotor and the superconductor, to find  $[J_{\phi_{sc}}^t]$ . And so, it is possible to write:

$$[ERROR]_{N \times 1}^t = [E_{EC}]_{N \times 1}^t - [E_{AV}]_{N \times 1}^t. \quad (10)$$

To solve equation 10 it must be defined a convergence criteria  $\epsilon$ , by the way that all the terms of  $[ERROR]_{N \times 1}^t$  must be smaller than a predefined constant  $\epsilon$  in order to reach the convergence to time  $t$ . This algorithm looks all the terms of  $[ERROR]_{N \times 1}^t = [error_1, error_2, \dots, error_k, \dots, error_{N-1}, error_N]$  and find the highest magnitude k-esime element in  $[ERROR]$ . For this element of index  $k$ , it is iteratively calculated an element  $\Delta J_{sc}$  and it is updated the current density in the element ( $J_{sc\ k} + \Delta J_{sc}$ ) until the condition  $|error_k| = error < \epsilon$  is true. This procedure is repeated in time  $t$  (for all N elements) until  $max|[ERROR]_{N \times 1}^t| < \epsilon$ . When the convergence is reached, it is known  $[J_{sc}]^t$  and it starts a new position of the magnetic rotor, that means, the instant  $t + \Delta t$ . It is important to observe that for the elements where  $|J_{sc}| = J_c$ , it has  $E_{AV} = E_{EC} = E_{\phi}$ , and the  $error$  on this element is null. The complete algorithm for this solution is presented on figure 2.

The levitation force can be calculated using Lorentz Force Law in the HTS elements:

$$F_y = \int_V J_{\phi_{sc}} \times B_{\rho\ tot} dV, \quad (11)$$

where  $V$  is the HTS volume and  $B_{\rho\ tot}$  is the magnetic flux density ( $ext + sc$ ) in the radial direction.

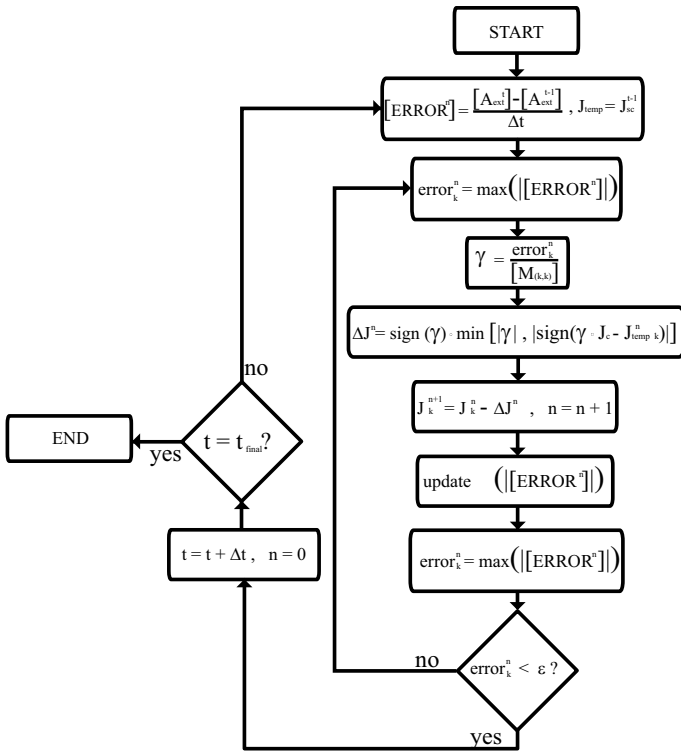


Fig. 2. Fluxogram applied to calculate  $J_{sc}$  in the superconductor.

### III. SIMULATION OF SIMPLE GEOMETRY

This section presents the application of the simulation model to a simple geometry. To estimate the quality of the YBCO sample, it is trapped a magnetic field inside the HTS. First it is applied a constant and homogeneous external field in the superconductor, and then the HTS bulk is cooled in  $LN_2$ . After that, the external field is removed and the trapped field is scanned. The results of the trapped field scanning for a HTS sample are presented on figure 3, for a vertical distance of 1mm from the surface of the sample.

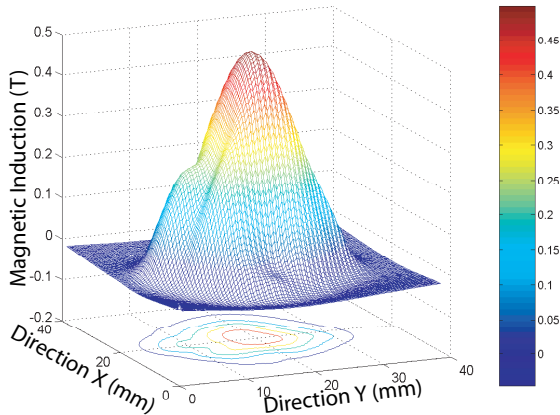


Fig. 3. Magnetic induction scanning of the trapped field in a sample of 28mm diameter at 77K. Applied field of 1.2T.

It was calculated the levitation force between the YBCO sample and a Nd-Fe-B magnet (with a diameter of 22mm, height of 10mm and coercivity force of 918kA/m), applying

the model describe above. Using an equivalent value of  $J_c = 1.8 \times 10^8 A/m^2$ , the levitation force was calculated and the results are presented in figure 4.

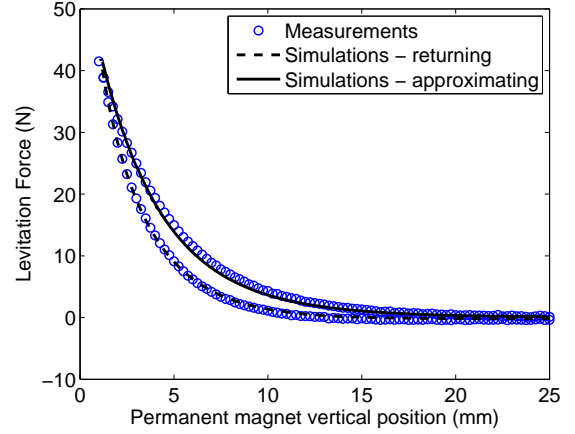


Fig. 4. Measured and calculated levitation force between a HTS and a permanent magnet for  $J_c = 1.8 \times 10^8 A/m^2$ .

## IV. SUPERCONDUCTOR MAGNETIC BEARING

### A. Magnetic Induction

Small scale thrust SMB prototypes were developed in this work to be used in future applications, such as high speed micro flywheels. The bearings are composed of a magnetic rotor (having approximately 80mm diameter and 15mm height) and a YBCO bulk of 75mm diameter and 16mm height). The two configuration of magnetic rotor are presented in figure 5, a flux shaper (FS) or flux collector and an axially magnetized ring (AMR) [7]. The YBCO disk used for the SMB is also shown in figure 5.

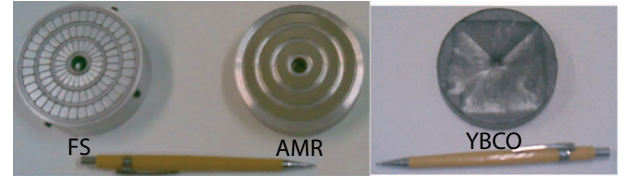


Fig. 5. Two types of magnetic rotors and YBCO bulk used for SMB.

The FS rotor configuration has three permanent magnets segmented rings magnetized radially. Between the magnet rings, there are some iron rings used to direct the magnetic flux. The AMR configuration presents three solid permanent magnet rings, magnetized axially and a back yoke (used to keep the magnets together and reduce the reluctance in one of the directions). The magnetic flux scanning for a distance of 3mm from the surface of the rotors are presented on figures 6 and 7, respectively for AMR and FS topologies. These two magnetic rotors configurations were compared in previous work [7].

### B. Simulation of levitation force for zero field cooling

In this section, the model described before to simulate the superconductor is applied to calculate the levitation force for

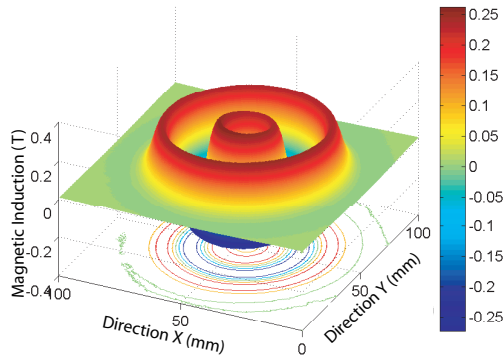


Fig. 6. Magnetic induction scanning of AMR rotor.

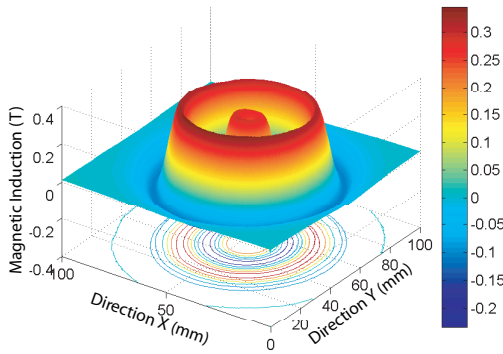


Fig. 7. Magnetic induction scanning of FS rotor.

the two SMBs prototypes constructed. As the SMBs rotor present more complex geometries, this simulation model fits well to do this task. Because the 75mm diameter YBCO  $J_c$  was not calculated, it was used a value of  $1.2 \times 10^8 A/m^2$ , obtained by trial and error. The results for the levitation force of topologies AMR and FS are presented in figures 8 and 9, respectively.

The simulations and measurements presented more agreement for the AMR than the FS configuration, for the adopted  $J_c$ . In the applied model, it were considered that the sample presents the same  $J_c$  in the whole section. It can be observed on figure 5, that the YBCO disc did not present homogeneity in the crystal grow for larger distances from its center and height.

## V. CONCLUSION

This work presented simulations and measurements of vertical levitation force in a SMB. When the model is applied to calculate the levitation force between a HTS cylinder and a permanent magnet, the maximum relative error was inferior to 5%, if an equivalent  $J_c$  was considered. For the calculation of the levitation force in SMB, the convergence during approximation presented the maximum error inferior to 8.5% and 20% for AMR and FS topologies, respectively. For the return movement, the convergence between simulation and measurement was not so close.

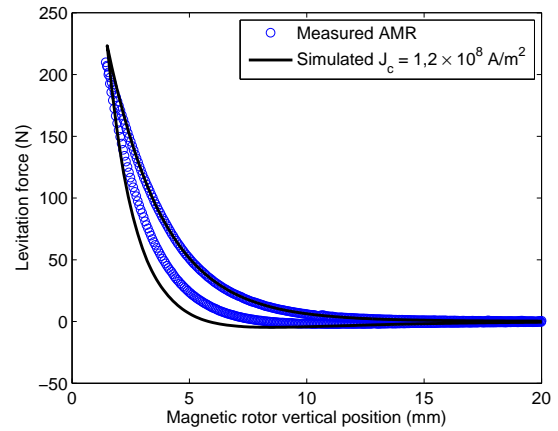


Fig. 8. Levitation force measured and simulated for the SMB using the AMR rotor.

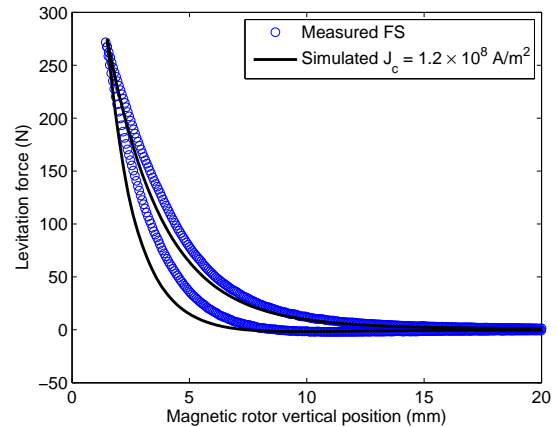


Fig. 9. Levitation force measured and simulated for the SMB using the FS rotor.

## REFERENCES

- [1] J. R. Hull, "Superconducting Bearings," *Superconductor and Science Technology*, 2000, vol. 13, pp. R1-R15.
- [2] G. G. Sotelo, "Modelagem de Supercondutores Aplicada ao Projeto de Mancais Magnéticos," *Ph.D thesis* (in portuguese), Federal University of Rio de Janeiro, 2007, Brazil.
- [3] C. P. Bean, "Magnetization of high-field superconductors", *Reviews of Modern Physics*, 1964, v. 9, pp. 31-39.
- [4] P. W. Anderson and Y. B. Kim, "Hard Superconductivity: Theory of the Motion of Abrikosov Flux Lines", *Reviews of Modern Physics*, 1964, v. 9, pp. 39-43.
- [5] T. Sugiura, H. Hashizume and K. Miya, "Numerical electromagnetic field analysis of type-II superconductors", *International Journal of applied Electromagnetics in Materials*, 1991, v. 2, pp. 183-196.
- [6] D. Ruiz-Alonso, T. A. Coombs, and A. M. Campbell, "Numerical Analysis of High-Temperature Superconductors With the Critical-State Model", *IEEE Transactions on Applied Superconductivity*, 2004, vol. 14 (4), pp. 2053-2063.
- [7] G. G. Sotelo, A. C. Ferreira, and R. de Andrade Jr., "Magnetic bearing sets for a flywheel system," *IEEE Transactions on Applied Superconductivity*, 2007, vol. 17 (2), pp. 2150-2153.
- [8] G. Barnes, M. McCulloch, and D. Dew-Hughes, Computer modeling of type II superconductors in applications," *Supercond. Sci. Technol.*, 1999, vol. 12, pp. 518522.
- [9] M. N. O. Sadiku, *Numerical techniques in Eletromagnetics*. EUA: CRC Press, 2<sup>nd</sup> ed., 2001.